Clinical Imaging 55 (2019) 8–11

Contents lists available at ScienceDirect

Clinical Imaging

journal homepage: www.elsevier.com/locate/clinimag

Body Imaging

Microvascular volume visualization utilizing computed tomographic angiography data facilitates resection of a complicated massive congenital hemangioma☆

Michael Winkler[a,d,*], Sherry Bayliff[b], Mohamed Issa[a], John Draus[c], Driss Raissi[a]

[a] Department of Radiology, University of Kentucky Chandler Medical Center, Lexington, KY, United States of America
[b] Department of Pediatrics, Division of Pediatric Hematology/Oncology, University of Kentucky Chandler Medical Center, Lexington, KY, United States of America
[c] Department of Surgery, Division of Pediatric Surgery, University of Kentucky Chandler Medical Center, Lexington, KY, United States of America
[d] Department of Internal Medicine, Division of Cardiovascular Medicine, University of Kentucky Chandler Medical Center, Lexington, KY, United States of America

ARTICLE INFO

Keywords:
Computed tomographic angiography
Congenital hemangioma
Post processing
Preoperative planning
Microvascular
Volume visualization

ABSTRACT

CT angiography (CTA) can be used for planning procedural and operative therapies for neonatal vascular lesions, such as congenital hemangiomas (CH), that are too morbid for medical therapy. Neonatal anatomy can be displayed within a small enough field-of-view that the nominal resolution of a modern CT scanner can be realized with a standard 512 × 512 storage matrix, yielding isometric ultrahigh resolution data and allowing for microvascular volume visualization. This case report details the creation and use of microvascular volume visualizations of CTA data during pre-procedural planning for treatment of this pathological entity.

1. Introduction

Most Congenital Hemangiomas (CH) are managed conservatively [1]. However, due to lesion necrosis, consumptive coagulopathy, or heart failure, a minority of CH require surgery. Given the patho-anatomical complexity of these lesions, preoperative imaging and embolization can be critical for therapeutic success [1].

Historically, computed tomographic angiography (CTA), which requires the use of ionizing radiation, has been avoided in these patients. However, with the advent of ultra-low radiation dose (ULRD) scanners, CTA has emerged as a first line tool for preoperative planning, especially when embolization is anticipated [2,3]. One advantage of CTA is that high quality microvascular volume visualizations (MVV) can be generated from CTA data, which consistently exhibits fine spatial resolution and isometry.

Herein we present a case of a tiny infant with a massive CH requiring both embolization and resection. The case exemplifies the advantages of CTA in pre-procedural planning for treatment of this entity. We applied several easy-to-master data processing techniques to create MVV from CTA data acquired with minimal radiation.

1.1. Case history

At one month of age, a male 3000 g infant with a massive CH of the left hemipelvis returned to the hospital with declining respiratory function. Echocardiography revealed high output heart failure. During pre-surgical assessment, the following concerns were raised: 1) the CH might extend into the pelvic cavity and involve the vasculature of the pelvic organs, 2) intraoperative bleeding might be impossible to control, and 3) the patient's small body habitus would make presurgical embolization lengthy and technically challenging. To address these issues, a CTA with MVV was requested.

2. Methods

2.1. Multiphase computed tomographic angiography

Multiphase CTA of the pelvis and proximal lower extremities was performed with a Somatom Force Scanner (Siemens, Forchheim, Germany) using an ULRD protocol (four helical scans at kVp 70 with reference mAs of 50). 20 ml of Iohexol (Omnipaque, GE Healthcare, Piscataway, New Jersey, USA) 350 mgI/ml contrast media was administered by hand injection. The scanner measured a dose-length

☆ This research did not receive any specific grant from funding agencies in the public, commercial, or not-for-profit sectors

* Corresponding author at: Thoracic and Cardiovascular Radiology, University of Kentucky, UK HealthCare Enterprise, 800 Rose Street, Room HX-313A, Lexington, KY 40536-0293, United States of America.
E-mail addresses: michael.winkler@usamobility.net, michael.winkler@uky.edu (M. Winkler).

https://doi.org/10.1016/j.clinimag.2019.01.015
Received 29 November 2017; Received in revised form 28 December 2018; Accepted 16 January 2019

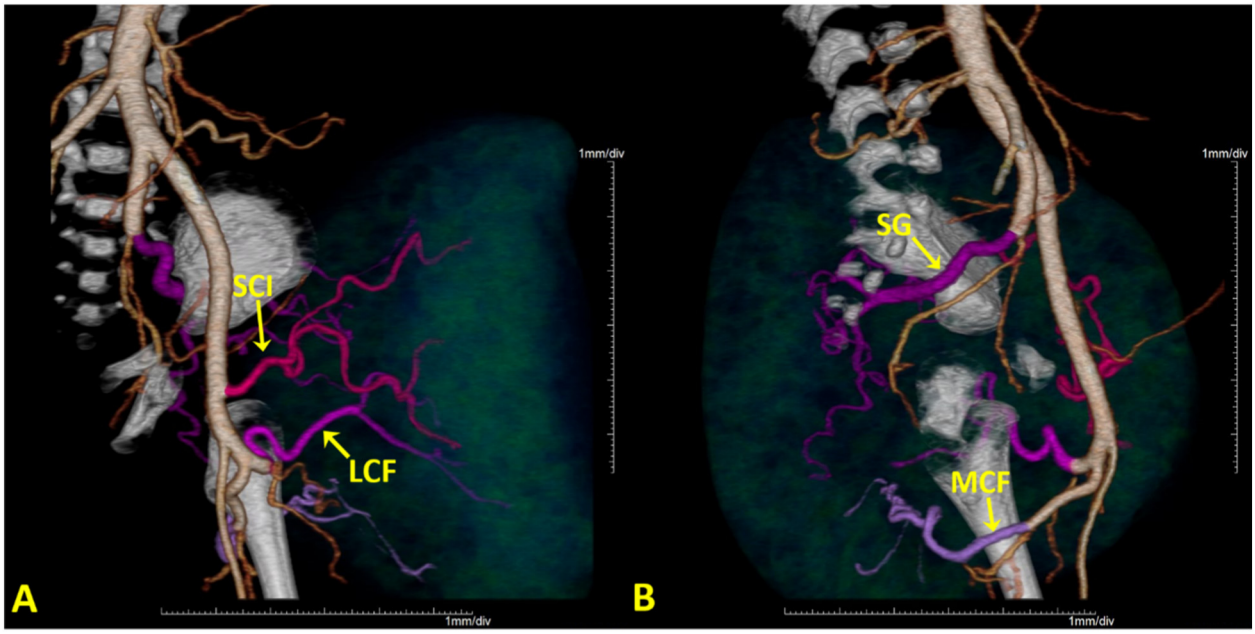

Fig. 1. Microvascular volume visualization of the left iliofemoral artery and its branches. The branch arteries which subserve the CH are color coded and labeled as follows: purple, SG = superior gluteal; magenta, SCI = superficial circumflex iliac; pink, LCF = lateral circumflex femoral; mauve, MCF = medial circumflex femoral. The aorta, iliofemoral arteries, and branch arteries other than those mentioned above are depicted in pale orange. The CH is rendered in translucent blue-green. (For interpretation of the references to color in this figure legend, the reader is referred to the web version of this article.)

product (DLP) of 49 mGy∗cm.

Special reconstructions were created from the best phase data using a limited 100 mm displayed field of view (FOV), 0.5 mm slice thickness, and a reconstruction interval of 0.1 mm. Model based iterative reconstruction (ADMIRE, Siemens, Forchheim, Germany) was maximized (level 5). These images were loaded into Intuition software (Terarecon, Foster City, California, USA). Sub-voxel sampling in the z-axis domain occurred automatically within the software, reducing the z-axis dimension of the voxels to 0.1 mm. Image post processing techniques of segmentation, pseudo-color multi-masking, and ray casting were performed to create MVV. Both still images (Fig. 1) and cine clips (Cine 1) were created for review.

2.2. Preoperative embolization

The MVV generated from the CTA were studied prior to and referenced during the embolization procedure by the interventional radiologist (IR). Right common femoral artery access was secured with a 4 Fr sheath. A 4 Fr catheter was advanced into the left common iliac artery. A microcatheter was used to selectively embolize, in sequence, the left superior gluteal, circumflexiliac, and lateral circumflex femoral arteries (Fig. 2). Each was embolized with 250-355 μm polyvinyl alcohol particles, supplemented with 500 μm Embozene particles (Boston Scientific, Marlborough, Massachusetts, USA) until stasis was achieved. The measured kerma-area product was 0.0015 Gy∗cm^2.

3. Results

Post operatively the patient's coagulopathy and high output cardiac failure resolved. His post-operative course was uneventful.

4. Discussion

4.1. Technique

Timing of CTA contrast injection in infants can be challenging; their cardiac output is high and each infant IV access has a unique tolerance for pressure which can only be determined “on-the-fly” by haptic feedback. Imaging low resistance vascular anomalies adds another layer of complexity. In this case rapid successive scans were performed to ensure acquisition of optimal data. The scanner's ULRD protocol limited the DLP of the exam to 49 mGy∗cm in spite of the fact that four phases were acquired. This value equates to an estimated effective dose of only 0.7 mSv using the abdomen/pelvis conversion factor of 0.015. This is only about half of the average annual background radiation of 1.3 mSv.

To achieve the best quality MVVs, several processing techniques were utilized.

A very small FOV was used during image reconstruction. The nominal in-plane resolution of the scanner is 0.24 mm by 0.24 mm. Because the standard storage matrix for CTA images is 512 × 512 [4], the true resolution of the scanner can only be demonstrated by reconstructed images less than or equal to 512 mm × 0.24 mm on a side. Thus, a FOV of 100 mm allowed for realization of the nominal resolution and a small amount of data enhancement by interpolation [4].

The reconstruction interval and the slice thickness were set as low as possible, 0.1 mm and 0.5 mm respectively. When reconstructed from helical projection data, axial images can be made to overlap, forcing “sub-voxel sampling” by advanced post processing software. The Hounsfield units (HU) of the sub-voxel samples sharing the same spacial coordinates are averaged, creating new smaller voxels that can be distinguished in HU from their immediate z-axis neighbors, thus improving the z-axis resolution of the data set [5].

Model based iterative reconstruction was maximized. ULRD scanning, small FOV reconstruction, and minimization of slice thickness and interval are all techniques that increase high spatial frequency noise, making segmentation during post processing more challenging. Without the aid of iterative reconstruction, the noise caused by these techniques would have made segmentation nearly impossible.

Manual and automated segmentation techniques were utilized to produce the MVV. Without a human operator to guide segmentation and discern artifacts from true anatomy, segmentation of submillimeter in diameter arteries would have failed. Data were segmented using both region of interest (ROI) growing and free hand ROI editing of multiplanar and maximum intensity images, as well as the draft volume

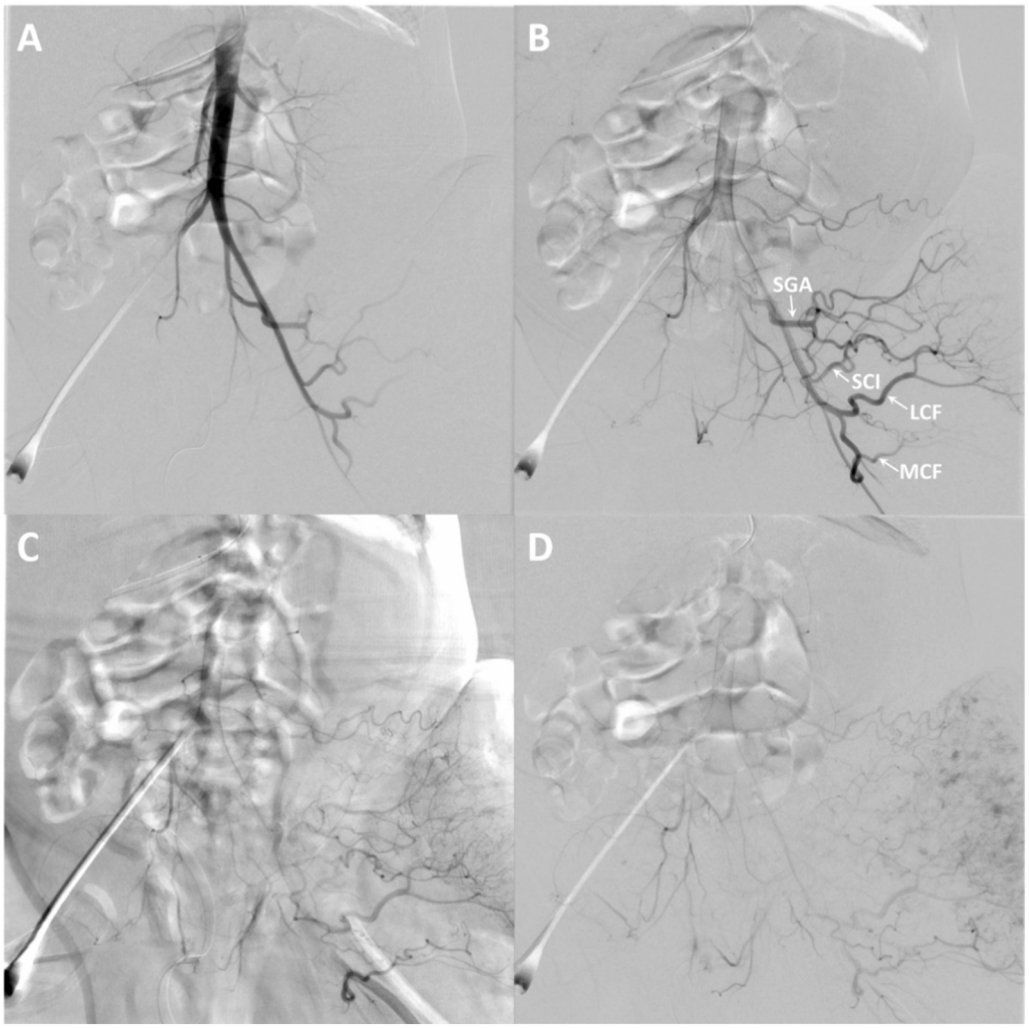

Fig. 2. Digital subtraction angiographic images of the left iliofemoral artery and its branches. Images depict early through late arterial phases. Branch arteries subserving the HC are demarcated with arrows and labeled as follows: SGA = superior gluteal artery; SCI = superficial circumflex iliac; LCF = lateral circumflex femoral; MCF = medial circumflex femoral.

rendered images themselves. Multiple segmentations (or masks), each with a different pseudocolor transfer function set, were utilized for each vessel of interest.

4.2. Implications for care

By representing the arterial tree of the lesion volumetrically, with different colors each representative of a different target for embolization, the MVV gave the IR foreknowledge of three-dimensional vascular anatomy. By virtue of comparison to the MVV, the initial intraprocedural conventional angiogram, despite complex vessel overlap, became immediately comprehensible. In addition, selective angiography of the visceral branches of the hypogastric artery was not needed to exclude pelvic organ involvement, since the CTA MVV images had excluded any involvement beforehand.

As a consequence, the IR needed only one angiographic projection to perform the embolization procedure, which he opined significantly minimized radiation exposure with a measured kerma-area product of only 0.0015 $Gy*cm^2$.

5. Conclusion

Although we have not performed a systematic study of the clinical impact of our MVV CTA reconstruction techniques, we believe they may play an important role in the management of challenging clinical situations similar to this case of a 3000 g infant with CH. A prospective trial withholding this benign technique we find hard to conceive, but it may be possible to study MVV techniques systematically in the future using propensity scored historical cases as comparisons.

Supplementary data to this article can be found online at https://doi.org/10.1016/j.clinimag.2019.01.015.

Acknowledgments

Drs. Abdulnasser Alhajeri, James Liau, Conor Lowry, and Douglas Schneider also participated in the multidisciplinary team care of the patient whose treatment course is detailed herein.

References

[1] Luu M, Frieden IJ. Haemangioma: clinical course, complications and management. Br J Dermatol 2013 Jul;169(1):20–30. https://doi.org/10.1111/bjd.1243623701395.
[2] Chen H, Lin X, Jin Y, Fan X, Li W, Ma G, et al. Deep infantile hemangiomas and early venous malformations: differential diagnosis by 3D CT angiography. Ann Plast Surg 2010 Jun;64(6):755–8. https://doi.org/10.1097/SAP.0b013e3181a72f3c20335793.
[3] Bittles MA, Sidhu MK, Sze RW, Finn LS, Ghioni V, Perkins JA. Multidetector CT angiography of pediatric vascular malformations and hemangiomas: utility of 3-D reformatting in differential diagnosis. Pediatr Radiol 2005 Nov;35(11):1100–6. https://doi.org/10.1007/s00247-005-1553-016041580.
[4] Mahesh M, Cody DD. Physics of cardiac imaging with multiple-row detector CT.

Radiographics 2007;27:1495–509. https://doi.org/10.1148/rg.27507504517848705.
[5] Kasales CJ, Hopper KD, Ariola DN, TenHave TR, Meilstrup JW, Mahraj RP, et al. Reconstructed helical CT scans: improvement in z-axis resolution compared with overlapped and nonoverlapped conventional CT scans. Am J Roentgenol 1995;164:1281–4. https://doi.org/10.2214/ajr.164.5.77172487717248.